JOURNAL OF GEOPHYSICAL RESEARCH, VOL. 88, NO. C8, PAGES 4633–4650, MAY 30, 1983

Gulf Stream Meanders off North Carolina During Winter and Summer 1979

DAVID A. BROOKS

Department of Oceanography, Texas A&M University
College Station, Texas 77843

JOHN M. BANE, JR.

Marine Sciences Program and Department of Physics, The University of North Carolina at Chapel Hill
Chapel Hill, North Carolina 27514

Meanders produced most of the subtidal variability in the Gulf Stream off North Carolina during 1979. Recording instruments were moored in the lower half of the water column over the 200-m and 400-m isobaths for two periods of 4 months, one in the late winter and one in the late summer. In both seasons, the middepth current speed typically fluctuated between -50 cm s^{-1} and $+100$ cm s^{-1} about a 30 cm s^{-1} downstream mean. The velocity, temperature, and salinity fluctuations had a prominent weekly time scale in the winter, caused by the meandering stream. In the summer the weekly time scale was less prominent within a generally energetic 3- to 10-day period band. In both seasons, the meandering currents were nearly in phase vertically, and the meanders propagated downstream at ~40 km d^{-1}. Shallow, in-shore filaments of warm water, separated from the main stream by bands of cooler surface water, are often extruded from the Gulf Stream front during the shoreward-most phase (crest) of meanders. Countercurrents, or upstream flow reversals, often occur under the filaments, forming the shoreward limb of cyclonic frontal eddies which are associated with uplifted cool water found upstream of meander crests. The energy source of the meanders off North Carolina remains obscure. The meandering currents locally transferred their kinetic energy to the mean stream, at about the same rate in each season. The loss of energy is consistent with an asymmetry or skewness of the meander process, often seen in satellite images of the surface temperature. The meandering currents were unrelated to the local wind, or to its curl or divergence, in either season. These results collectively point to an upstream source of meander energy, most probably made available by an instability of the Gulf Stream.

1. Historical Setting of the Gulf Stream Meanders Experiment

The variability of the Gulf Stream was appreciated soon after its discovery in 1513 by Ponce de León. His ships were swept northward along the southeastern Florida coast (Figure 1) by a 'current which was more powerful than the wind' (*Herrera y Tordesillas* [1601]; also see *Scisco* [1913] for a detailed description of Ponce de León's track and Herrera's paraphrase of the expedition). The explorers initially encountered the current near what is now Jupiter Inlet and again near Lake Worth; on each occasion they were compelled to seek anchorage under the lee of a coastal cape because they could not stem the current offshore. Scisco suggested that the vessels 'waited for the [tidal] current to abate,' but this seems unlikely because the expedition remained at each anchorage for many days while occupied with other matters. Recent information indicates that the stream meanders laterally, at times bringing strong northward currents within a few kilometers of the southeastern Florida coast and at other times leaving the coastal waters relatively quiet. After leaving each anchorage, the expedition was able to continue its southward progress. Inadvertently, Ponce de León may have been the first to exploit Gulf Stream meanders.

In the latter half of the sixteenth century, a working knowledge of Gulf Stream eddies in the South Atlantic Bight (Figure 1) was available. John White's casual remark in 1590 about southward setting eddy currents along the Carolina coasts suggests the familiar nature of this information (see *Quinn* [1952] for the context in which White's remark was made). During the next two centuries, many observations were made in the Gulf Stream, and a number of theories were offered to explain its existence [*Stommel*, 1966]. Benjamin Franklin and William De Brahm have been credited with producing the first realistic charts of the Gulf Stream [*DeVorsey*, 1976], and copies of Franklin's original (1769) chart have only recently been rediscovered [*P. L. Richardson*, 1980].

Nineteenth century surveys in the South Atlantic Bight led to Bache's discovery in 1860 of cold water bands interleaved within the stream [*Pillsbury*, 1891]. *Pillsbury* [1891] showed that the interleaving was variable in time and position, and he attempted to relate Gulf Stream fluctuations to atmospheric and lunar effects. More recent studies [*von Arx et al.*, 1955; *Webster*, 1961*a*; *Lee et al.*, 1981] have shown that the interleaving process is associated with meandering, which produces warm filaments of surface water which are extruded from the inshore edge of the Gulf Stream and are separated from it by a cold water band. The warm filaments were called 'shingles' by von Arx et al. because they provided an overlapping structure of alternating warm and cold water along the inshore edge of the stream. Based on temperature measurements from repeated crossings of the stream, *Webster* [1961*a*] described the meanders as skewed, wavelike, lateral excursions of the mean stream. The meanders were observed to travel downstream, such that the temperature fluctuations at a fixed observation site had a prominent weekly time scale. The recent work by *Lee et al.* [1981] has given a detailed description of the three-dimensional structure of meanders and filaments off Georgia.

In 1979 we conducted a field study of Gulf Stream meanders off North Carolina (the boxed inset of Figure 1).

Paper number 2C1366.
0148-0227/83/002C-1366$05.00

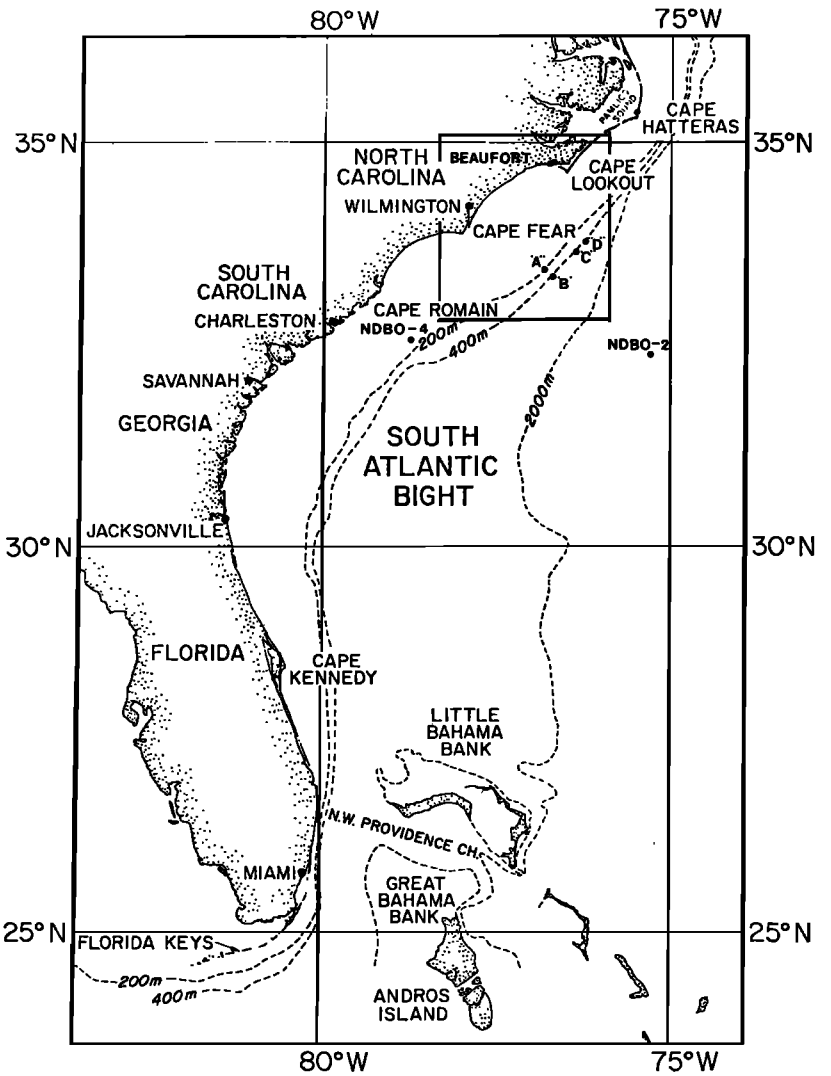

Fig. 1. Map of the South Atlantic Bight, showing the central study area (boxed inset). The locations of the four moorings are labelled A through D. Atmospheric observations were obtained at the NOAA Data Buoy Office offshore stations marked NDBO-4 and NDBO-2 and also at Cape Hatteras.

Subsurface moorings supporting two or three Aanderaa current meters each were maintained at sites A through D for two 4-month periods, one in the winter and one in the summer. The instruments were deployed in the Gulf Stream over the 200-m and 400-m isobaths, at nominal depths of 100 and 180 m at mooring A and at depths of 250, 320, and 380 m at the other moorings (320-m instrument omitted at mooring B). The winter observations have been summarized by *Brooks and Bane* [1981; referred to hereafter as BB81], who give more information about the mooring array design and the basic data processing techniques that were used. The field study included four hydrographic cruises and 13 aircraft air-dropped expendable bathythermograph (AXBT) surveys. The full set of observations is documented in a set of six data reports, the last of which is listed in the references [*Brooks et al.*, 1981].

In this paper we compare Gulf Stream fluctuations and meanders between Charleston and Cape Hatteras observed during the winter and summer periods. Previous direct observations of the Gulf Stream in this area [*Webster*, 1961*a*; *W. S. Richardson et al.*, 1969] have not permitted this comparison because of their relatively short duration. The seasonal perspective available from the Gulf Stream Meanders Experiment data set may help address some of the fundamental questions about the meander mechanism.

2. Basic Statistics of the Winter (January to May) and Summer (August to November) Observations

The mooring locations and the mean current vectors for the summer case are shown in Figure 2. The analogous mean winter currents are shown in BB81. The moorings were deployed in approximately the same location on the continental slope in both seasons. The current meter spacing provided measurements on scales of 11, 64, and 75 km in the downstream direction, 18 km cross stream, and 60–120 m vertically. The sampling interval was 20 min for all instruments. The edited data were smoothed with a 3-hour low-pass (3 HRLP) filter to reduce sampling noise. A 40-hour low-pass (40 HRLP) filter was then used to separate the fluctuations with periods longer than 40 hours from those of shorter periods. A Lanczos taper was used for both filters. The velocity components and vectors are presented in a

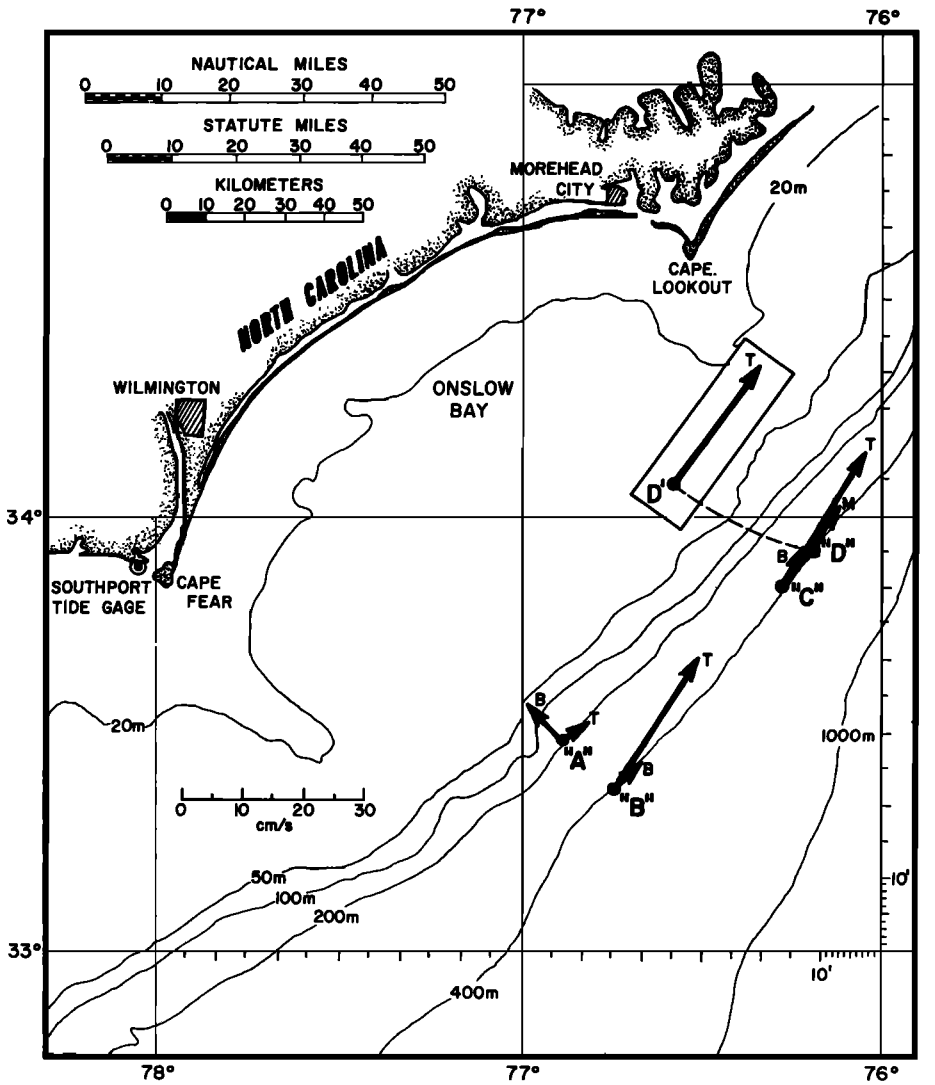

Fig. 2. Map of study area, showing mean current vectors for each instrument for the 4-month summer period. The vector for mooring D is displaced for clarity (inset box). The letters at the arrowheads identify top (T), middle (M), and bottom (B) instruments (see Table 1 for depths). The analogous winter mean vectors are given by *Brooks and Bane* [1981].

coordinate frame rotated 34° clockwise from true north to align with the local topography, such that the v component of the velocity vector is positive in the downstream direction and the u component is positive offshore. A comparison of the first-order statistics of the velocity components and water temperature at each instrument is given in Table 1.

In both seasons the mean flow was essentially in the downstream direction at all instruments, except for the near-bottom instrument on mooring A (A-bot). A shoreward mean flow component occurred at A-bot in the summer (−8 cm s^{-1}) and in the winter (−3 cm s^{-1}). The mean downstream (v) velocity components were generally slightly larger in the winter than in the summer. The standard error of the mean estimates, computed by dividing the standard deviation by the square root of the number of hourly values of the 3 HRLP records, is less than 1 cm s^{-1}.

In most cases, the range of the velocity component fluctuations was much larger than the corresponding mean, the extreme example being the summertime v component range of -86 to 126 cm s^{-1} relative to a mean of 5 cm s^{-1} at A-top. The standard deviations of the velocity components at a particular instrument show little seasonal difference, and the spatial distribution of the standard deviations was also similar in the two seasons.

The frequency distribution of the horizontal kinetic energy of the velocity fluctuations during the winter and summer seasons is shown in Figure 3 as summary velocity-component variance spectra. For each season the mean variance estimate for all the instruments in each frequency band is shown by the heavy lines. The thin lines show the extrema, and the shaded area covers one standard deviation relative to the means. In the winter, velocity component fluctuations with 7- to 10-day and 3- to 4-day time scales were prominent in the variance spectrum. The winter spectrum in Figure 3 is typical of Gulf Stream meanders as discussed by *Webster* [1961*a*]. In the summer the velocity component fluctuations had less well-defined time scales in a generally energetic 3- to 10-day period band. The peak value occurring near the 8-day period in each season differs significantly from adjacent estimates, since the standard error for the variance

TABLE 1. Winter/Summer Comparison of 3-Hour Low-Pass-Filtered Current Components (u, v; cm s^{-1}) and Temperature (T; °C) for Each Moored Instrument

Instrument (Depth, m)	Parameter	Minimum	Maximum	Mean	Standard Deviation
A-top	u	−39/−37	49/50	0/2	10/13
(98/100)	v	−71/−86	117/126	7/5	34/44
	T	13/12	24/24	17/18	2/2
A-bot	u	−32/−51	44/31	−3/−8	9/10
(178/180)	v	−59/−66	75/76	4/2	21/20
	T	4/*	20/*	12/*	3/*
B-top	u	−56/−59	64/48	1/−1	16/16
(250/270)	v	−50/−41	134/126	25/26	29/30
	T	9/9	19/17	13/12	3/2
B-bot	u	−34/−36	40/41	2/1	11/10
(370/390)	v	−63/−41	53/67	5/6	17/10
	T	6/6	14/12	9/8	2/1
C-top	u	−33/−38	54/36	4/1	12/10
(245/260)	v	−44/−57	135/139	32/25	34/34
	T	9/9	18/17	13/12	2/2
C-mid	u	−99/−30	83/37	0/0	16/9
(305/320)	v	−46/−56	113/113	23/17	27/27
	T	3/8	30/16	11/11	2/2
C-bot	u	−33/−24	48/29	−1/−1	10/8
(365/380)	v	−40/−50	74/63	9/8	20/19
	T	7/6	14/13	9/9	1/1
D-top	u	−28/−41	48/39	4/1	10/10
(236/250)	v	−35/−48	122/142	32/24	29/34
	T	9/9	19/17	13/12	2/2
D-mid	u	−30/*	42/*	−1/*	9/*
(296/310)	v	−46/*	116/*	24/*	29/*
	T	8/*	19/*	11/*	2/*
D-bot	u	−27/*	35/*	0/*	8/*
(356/370)	v	−38/*	55/*	8/*	17/*
	T	7/*	14/*	9/*	1/*

Instruments are identified by mooring letter (Figure 1), with an appended abbreviation indicating depth on the mooring. 'Winter' means January 16 to May 14, 1979, and 'summer' means August 1 to November 17, 1979. The water depth was nominally 200 m at the A mooring and 400 m at the others.
*No data.

estimated from the 10 instruments (8 in summer) is ~2 to 3 cm^2 s^{-2}. In both seasons the mean subtidal u component variance was about one-fifth of the v component variance. The tidal fluctuations in both seasons were primarily semidiurnal, and they were about twice as energetic in the u component as in the v component. The inertial period at the experiment latitude (~33°30'N) is 21.7 hours, but there is only inconclusive evidence of an inertial peak in the mean variance spectra in either season.

3. Subtidal Fluctuations

Seasonal differences in the subtidal fluctuation time scales are apparent in the full-length 40 HRLP records, shown for the B-top instrument in Figure 4. The 7- to 10-day time scale is prominent in the winter velocity, temperature, and salinity, especially during the first and last thirds of the record. In the summer the band of energetic fluctuations extended to noticeably shorter periods of 3 or 4 days, which is consistent with the mean variance distribution for the entire array (Figure 3).

The weekly time scale fluctuations at B-top abated in late February and did not resume until March 29 (Figure 4*a*). The absence of the v component reversals associated with meandering makes this quiescent period stand out in the winter velocity-vector time series. The 3- to 4-day period fluctuations are relatively more noticeable during the quiescent period. The velocity, temperature, and salinity decreased slowly during March, suggesting that the stream gradually moved offshore of the array area. The surface temperature structure from the week prior to the March 29 meander indicates that the stream, or at least its surface manifestation, was located unusually far offshore during late March [*Hood and Bane*, 1983]. The March 29 meander, which ended the quiescent period, produced the largest downstream current speed of either season at B-top (134 cm s^{-1}).

A period of relatively small amplitude fluctuations also occurred during the summer (mid-September to mid-October, Figure 4*b*). However, this period is distinguished mainly by a reduction in the amplitude of the fluctuations, and not by a change of their period or an absence of v component reversals, as occurred in the winter.

In both seasons the v component of velocity, temperature, salinity, and the $\partial v/\partial x$ horizontal velocity shear term fluctuated nearly in phase (Figure 4). The $\partial v/\partial x$ term was calculated from the middepth current meters on the A and B moorings, and, to estimate the relative vorticity, the $-\partial u/\partial y$ term was calculated from the middepth current meters on the C and D moorings. The $-\partial u/\partial y$ term was given an artificial time lead of 39 (38) hours in the winter (summer) to account for the mean downstream propagation speed of the meanders. The resulting time series of relative vorticity components can be viewed as middepth estimates in a 15 km × 15 km box centered between the A and B moorings. Cyclonic rotation of the velocity vectors (leading phase of u with respect to v at a single instrument, Figure 4) and positive peaks in $\partial v/\partial x$ are characteristic features of meanders which occur at a fixed site shortly after the passage of meander crests. (We define a meander crest to be the local, shoreward-most displacement of the Gulf Stream front.) These characteristics have been discussed by BB81 for the large-

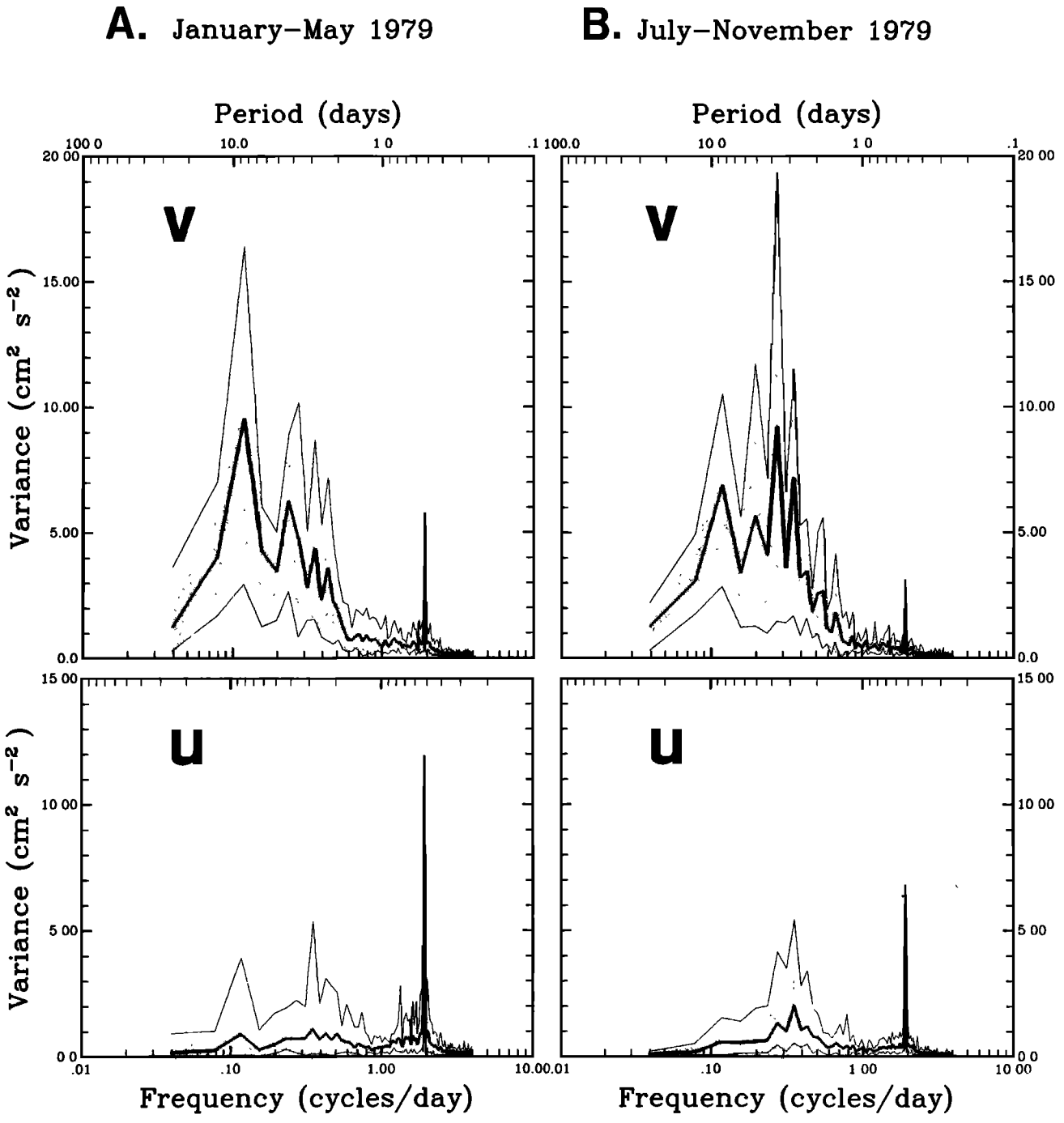

Fig. 3. Frequency distribution of the current component variance, for the (*a*) winter and (*b*) summer periods. The downstream component (v) is aligned with the local bottom topography (34°T), and the u component is offshore. The heavy lines show the mean variance estimate in each frequency band for all the instruments. The thin lines show the corresponding maxima and minima, and the shaded area covers one standard deviation in each band. The mean variance estimates have about 20 degrees of freedom in each band.

amplitude meander which occurred on March 29 and by *Bane et al.* [1981; referred to hereafter as BBL] for the meanders which occurred on February 5 and 11. In both seasons the magnitude of the shear term $\partial v/\partial x$ occasionally approached the local value of the Coriolis parameter (f), which is equal to 8.2×10^{-5} s^{-1} at 34° latitude. During most of the meanders, the $-\partial u/\partial y$ term was smaller than and tended to be out of phase with the $\partial v/\partial x$ term, but an exception occurred during the March 29 meander. During that event the terms in the relative vorticity, $\zeta = \partial v/\partial x - \partial u/\partial y$, were of about equal magnitude and they had the same sign, leading to the largest value of ζ during the entire field study. As noted in BB81, the March 29 meander occurred as the stream moved shoreward over the moorings, ending a month-long period of unusually low meandering activity. The relatively large positive relative vorticity which occurred during the March 29 meander may be an indication of the onshore orientation of the mean stream at the end of the quiescent period.

The effects of several large meanders are evident in Figure 4*b* during the first few weeks of the summer B-top records. The same meanders were also responsible for large-ampli-

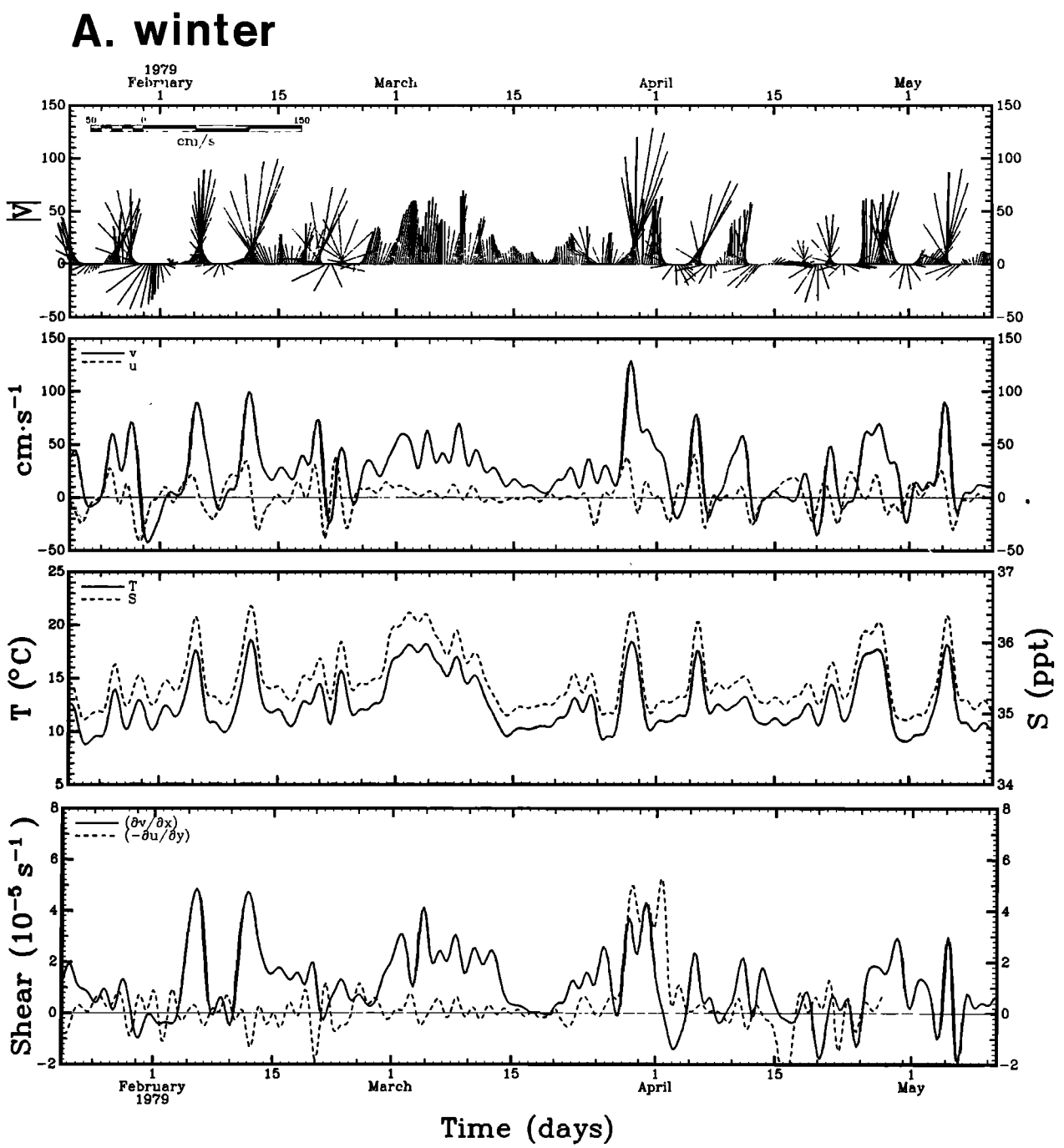

Fig. 4*a*. Full-length, 40-hour low-pass-filtered records of velocity vectors and components (v, u), temperature (T), and salinity (S) from the B-top instrument during winter. Velocity vectors (top panel) pointing toward the top of the figure correspond to downstream flow. The bottom panel shows the relative vorticity components due to horizontal velocity shear, estimated from the moored array (see text). The $-\partial u/\partial y$ term has been shifted to the left by 39 hours tc account for the mean downstream propagation speed of the fluctuations.

tude fluctuations at the A-top instrument during the first 30 days of the summer mooring period (Figure 5). This figure can be directly compared with Figure 2 in BB81, which shows the same information for the first 30 days of the winter mooring period. In both seasons, the v, T and S increases were almost in phase, and the u increases lead the v increases by less than one quarter of a meander period. These phase relationships imply an offshore flux of heat and momentum. It can also be seen in Figure 5 that increases in v, which occur during the approaching phase of a meander crest, generally last longer than the decreases in v, which occur after the crest passes. This asymmetry was pointed out by BB81 for the winter case, and it appears to be a meander characteristic which is independent of season. The sense of the observed meander skewness (a relatively gentle approach of the Gulf Stream front, followed by an abrupt offshore displacement of the front after the crest passes) is consistent with *Webster*'s [1961*a*] description of the temperature field skewness that he observed in the upper 200 m. The skewness sense and our computed momentum fluxes are also consistent with a local conversion of meander kinetic energy to mean stream kinetic energy, a surprising

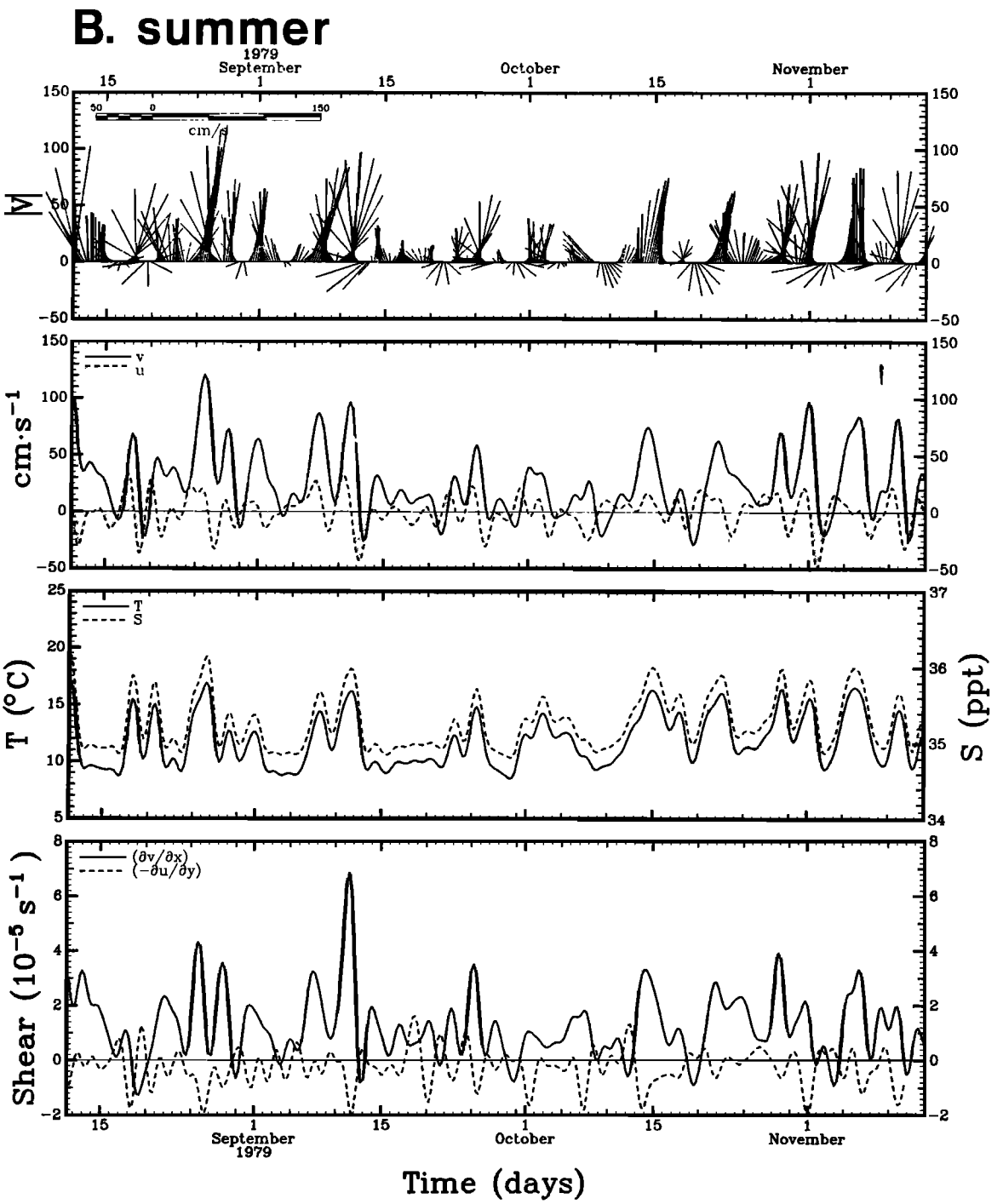

Fig. 4*b*. Full-length, 40-hour low-pass-filtered records of velocity vectors and components (v, u), temperature (T), and salinity (S) from the B-top instrument during summer. Velocity vectors (top panel) pointing toward the top of the figure correspond to downstream flow. The bottom panel shows the relative vorticity components due to horizontal velocity shear, estimated from the moored array (see text). The $-\partial u/\partial y$ term has been shifted to the left by 38 hours to account for the mean downstream propagation speed of the fluctuations.

result first noted for the surface layer by *Webster* [1961*b*].

The three large v component peaks at A-top (Figure 5) associated with the meanders that occurred on August 11, 18, and 26 appeared 36, 30, and 33 hours later, respectively, at the C-top instrument (Figure 6). Over the 64 km separating the downstream C mooring from the A-to-B line, the time delays give phase propagation speeds of 43, 51, and 47 km d^{-1}, respectively. These estimates of the summer phase speed can be compared with a mean wintertime estimate of 40 km d^{-1} deduced from satellite images of the stream's surface thermal front [*Legeckis*, 1979], and with estimates ranging from 30 to 45 km d^{-1} for individual winter meanders [BB81, BBL]. Averaged over the full record lengths, lagged correlations between the v components at B-top and C-top lead to estimates of the mean downstream phase speed of about 40 km d^{-1} for both seasons [*Ignaszewski*, 1982].

The subtidal fluctuations were highly correlated and vertically in phase during the summer at mooring C, as shown in Figure 6 for the first 30 days of the record. A similar situation existed in the winter [BB81], when satellite images of the

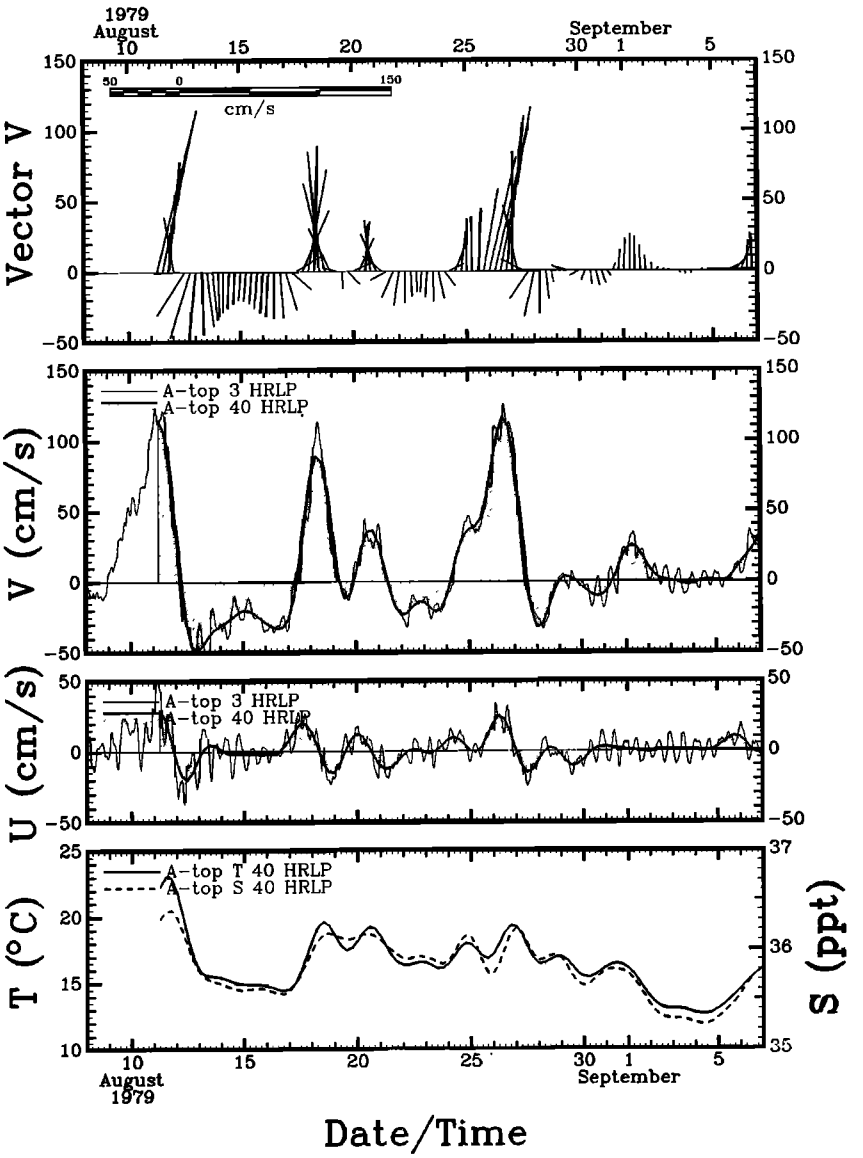

Fig. 5. Velocity vectors and velocity components (v, u), temperature (T), and salinity (S) from the A-top instrument during the first 30 days of the summer experiment. The effects of three meanders are prominent. This figure can be directly compared with Figure 2 in the work of *Brooks and Bane* [1981] for the winter case. The vector convention is the same as Figure 4. Thin lines show 3-hour low-pass-filtered data and heavy lines (solid and broken) show 40-hour low-pass-filtered data.

surface temperature structure showed that the deep velocity fluctuations were also highly correlated with the stream's meandering surface thermal front. In both seasons the high vertical coherence and the in-phase nature of the fluctuations are consistent with a simple oscillatory lateral translation of the subsurface Gulf Stream front over the array site, as *Webster* [1961*a*] originally suggested. Detailed AXBT surveys of meanders passing through the array area support this zero-order kinematic interpretation, but a more complicated vertical structure is apparent along the inshore edge of the stream and upstream of the study area [BBL].

Periods of upstream flow, or countercurrents, are correlated with the passage over the array of warm filaments found along the inshore edge of the stream [BB81; BBL; *Lee et al.*, 1981]. The filaments are elongated bands of surface Gulf Stream water that are extruded from and trail southwestward of meander crests. The warmness of filaments is primarily a surface feature, confined to the upper few tens of meters, but the countercurrents associated with them are deeper features associated with upwarping of the isotherms along the inshore Gulf Stream front during the offshore displacement phase of a meander. Thus at the 100-m depth over the 200-m isobath, for example, the countercurrents following the passages of meander crests are associated with decreasing temperature and salinity (Figure 5). Figure 7 shows a winter example of a temperature section through a warm filament on the inshore edge of the stream, taken about 20 km upstream of a meander crest. The cold surface water separating the filament from the main stream is clearly evident, and isotherm uplifting under the cold surface water defines a 'cool core' that extends to near bottom. The cold surface water bands noted by Bache and Pillsbury [*Pillsbury*, 1891] and the southward setting 'eddie currents' mentioned by John White in 1590 were probably similar manifestations of meanders.

The countercurrents form the shoreward limb of the

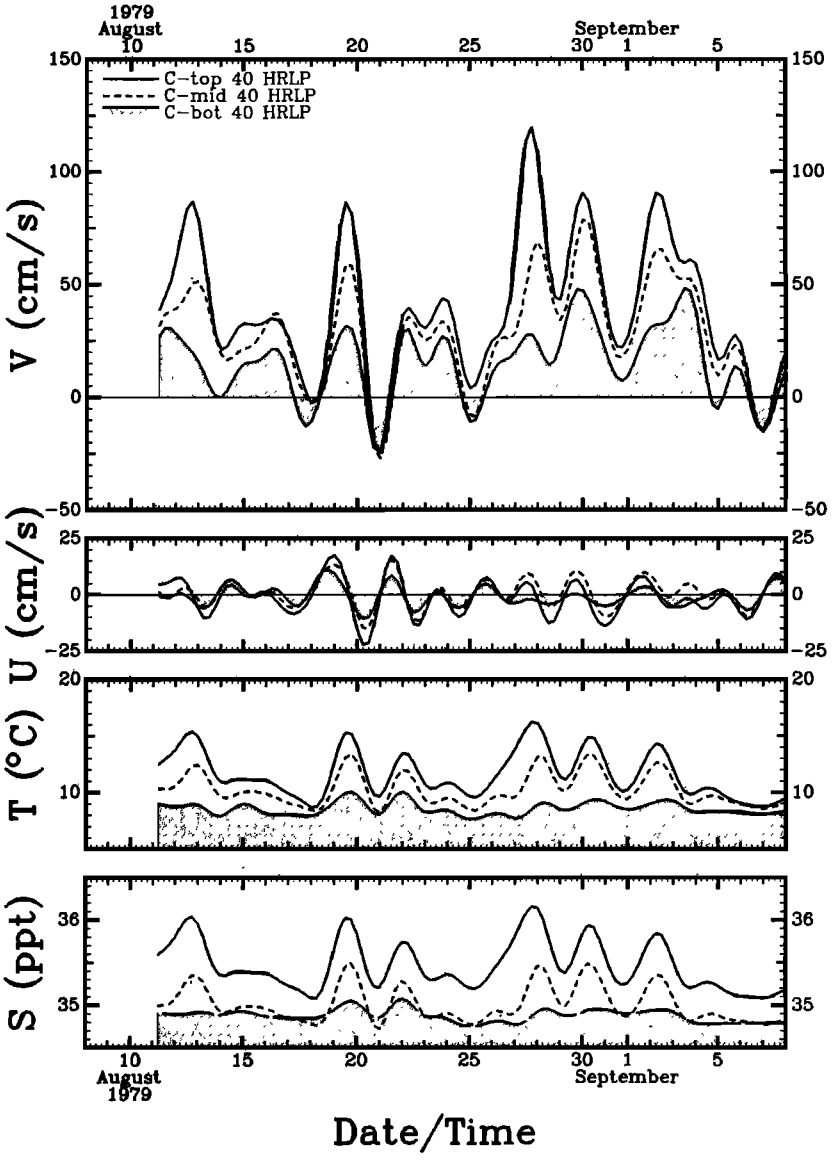

Fig. 6. Velocity components (v, u), temperature (T), and salinity (S) from the top, middle, and bottom instruments on mooring C during the first 30 days of the summer experiment. The high vertical coherence of the meandering currents is apparent.

cyclonic circulation around the upwarped isotherms, consistent with a geostrophic interpretation in which the density field is strongly temperature controlled. *Lee et al.* [1981] found the circulation around cool core frontal eddies to be nearly in geostrophic balance with the density structure. They also found that cyclonic circulation around cold core eddies provided a major part of the low-frequency current and temperature variability from Florida to Georgia. Their detailed description of 'frontal eddies' is very similar to ours for the region off North Carolina, with the exception that the amplitude of lateral excursion of the surface Gulf Stream front and the downstream extent of warm filaments are greater off North Carolina. The frontal excursion amplitude, determined from satellite images, increases rapidly downstream of Charleston, South Carolina, where a bottom feature often deflects the stream seaward [cf. *Bane and Brooks*, 1979]. The excursion reaches its largest amplitude off the southern end of Onslow Bay, then decreases downstream. This indicates an eddy growth period of only several days downstream of Charleston, compared with about a week upstream of Charleston [*Lee et al.*, 1981]. The rapid growth of a meander during the several days after it passes Charleston indicates that the deflection of the stream amplifies the frontal eddies that apparently originate upstream as unstable perturbations of the Gulf Stream front [*Lee et al.*, 1981]. By the time the meanders reached our mooring array in Onslow Bay, however, they appeared to be giving up their kinetic energy to the mean stream (cf. section 5).

Much of the information about the subtidal fluctuations can be conveniently summarized in a spectral representation. A comparison of spectra, coherence, and phase results keyed on the B-top instrument is given in Figure 8 for the winter and summer periods. Figure 8*a* shows selected autospectra for v at instruments separated in the cross-stream and downstream directions, Figure 8*b* shows the coherence and phase relations between v at instruments separated 64 km in the downstream direction, and Figure 8*c* shows the coherence, phase, and momentum flux relations between u and v at a single instrument.

The winter-to-summer change in the distribution of vari-

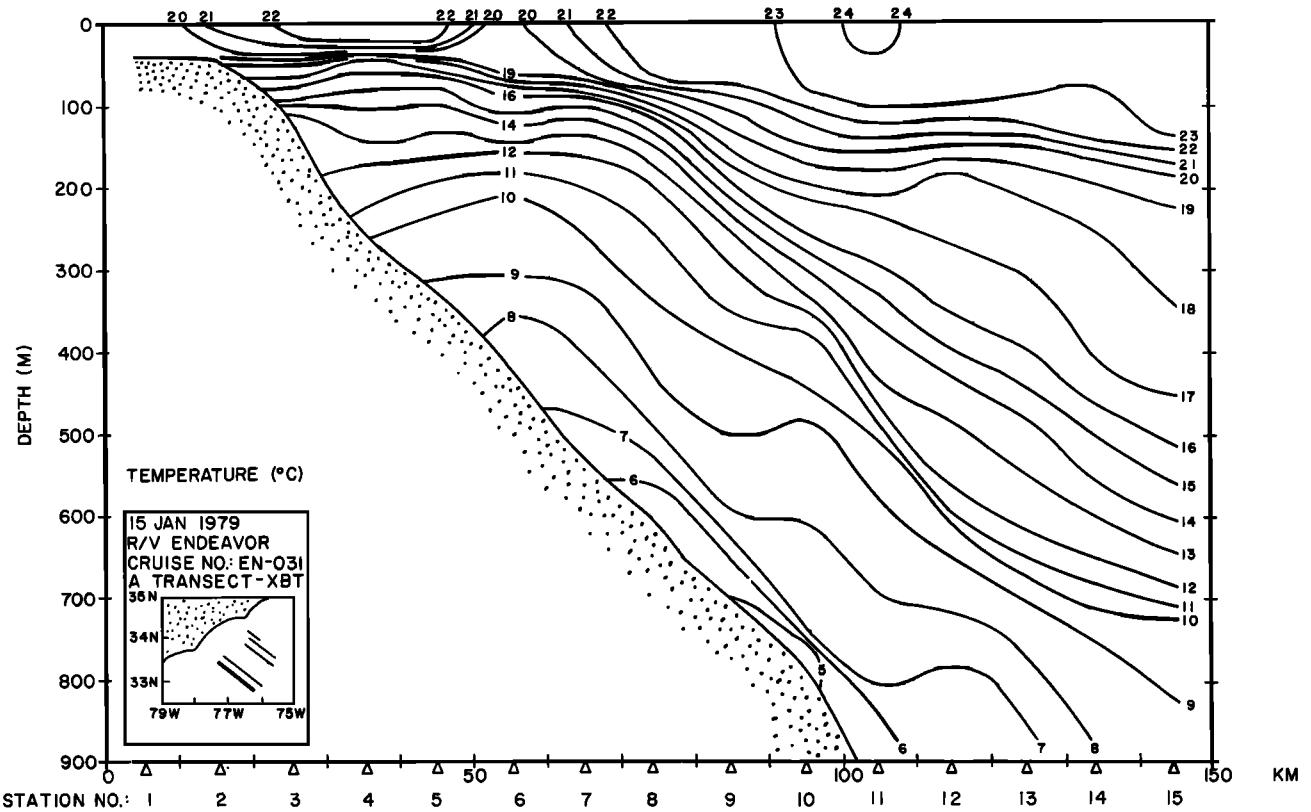

Fig. 7. A temperature section across the Gulf Stream, approximately along the line between the A and B moorings (inset). This winter example clearly shows the shallowness of a warm filament on the inshore edge of the main Gulf Stream front, and the relatively cold water separating the filament from the stream at the surface. The upwarping of isotherms under the cold surface water is associated with cyclonic rotation of the water after the meander crest passes over a fixed location. The section was taken about 20 km upstream of a meander crest.

ance noted earlier (Figures 3 and 4) is evident in the v autospectra (Figure 8*a*). In the winter, the dominance of the 7- to 10-day period fluctuations is emphasized by the relative lack of kinetic energy of motions with very long periods (>2 weeks). (The spectrum density estimates in Figure 8 are not artificially whitened, as they are in the variance-conserving format of Figure 3. Mean values were removed from the 40 HRLP data before calculating the spectrum densities, but no further filtering or spectrum weighting was performed.) In the summer, on the other hand, the spectrum densities generally increase for very long periods, which tends to mask the peak in the 7- to 10-day period band, especially for the C-top v component. The summer time spectrum redness is also apparent for the B-top and B-bot v components, which can be qualitatively confirmed for B-top in Figure 4*b*. The general organization of the fluctuations into two period bands, roughly 3 to 4 days and 7 to 10 days, was noted by *Webster* [1961*a*] for the near-surface layer temperature field. A similar organization is evident in Figure 8 for the near-bottom and middepth current fluctuations, although the relative spectrum density in the two bands depends on season and instrument location.

The fluctuations were coherent over the downstream scale of the array (64 km) for the period range of about 2 to 10 days, in both seasons (Figure 8*b*). In this period range, the summer coherence values were generally lower band for band than in the winter, except for the 3- to 4-day period band, which also stands out in the summer time series for v at B-top (Figure 4*b*). The summer increase in variance at very long periods (>2 weeks) is reflected in increasing downstream coherence at very long periods. The downstream phase propagation noted for the individual meanders in Figure 5 is a general feature of the coherent subtidal fluctuations. This is clearly evident in the sloping phase versus frequency graphs in Figure 8*b*. The mean slopes of the phase graphs are very similar, indicating a downstream phase speed of 43 km d^{-1} in each season for the coherent subtidal spectrum of fluctuations. Small differences in the structure of the two graphs may imply that the phase speeds were period dependent and seasonally dissimilar, but the statistical confidence in the phase estimates does not permit such a detailed comparison. (The 95% confidence interval on the phase estimate is about ±(3, 12, 18) degrees in a frequency band with a coherence squared estimate of (0.9, 0.8, 0.7).)

4. The Three-Dimensional Temperature Structure of Meanders

Conventional hydrographic surveys from a single vessel are too slow to adequately resolve the three-dimensional structure of Gulf Stream meanders off North Carolina. For this reason, two survey sequences of aircraft flights were made along the continental margin between Cape Hatteras and Charleston (Figure 1). Eight flights were made between February 9 and 18, and five flights were made between November 21 and 29. During each flight, AXBT's were dropped on a grid which included the moored instruments,

giving a quasi-synoptic, three-dimensional picture of the temperature field in the upper 400 m. Station spacing was nominally 12.5 km in the cross-stream direction and 50 km in the along-stream direction. Each AXBT survey required about 4 hours to complete, during which time the thermal expression of a Gulf Stream meander could be expected to move downstream under the survey by about 6.5 km. Further details concerning the survey technique and AXBT drop stations are given in BBL and in the sequence of data reports listed in the references.

Winter and summer examples of the AXBT views of the temperature field are shown for comparison in Figure 9 for surveys performed on February 11 and November 27. The February flight sequence occurred as two large meanders were propagating through the area. The v component signatures of these meanders are evident in Figure 4*a* on February 5 and 11, and their relation to the AXBT temperature field

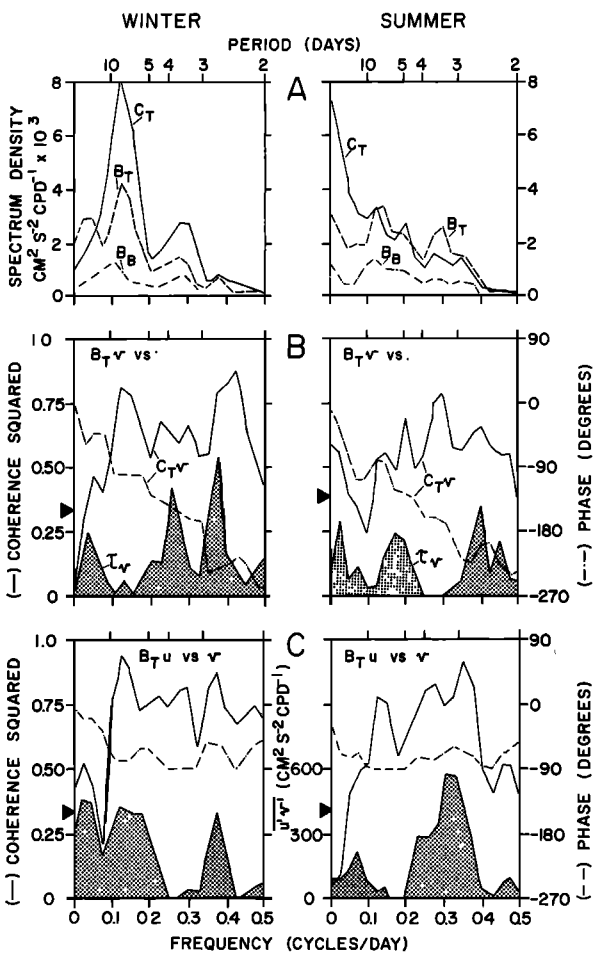

Fig. 8. Summary spectrum calculations keyed on the B-top current meter, for the winter and summer cases. (*a*) Autospectra of the v velocity components from selected instruments, permitting a vertical and a downstream comparison of the frequency structure of the fluctuations in each season. (*b*) The coherence and phase difference of the v component between the B-top and C-top instruments, and an example of the low coherence between the currents and the downstream wind stress (τ_v) at offshore buoy NDBO-2 (shaded area). (*c*) High coherence and near-quadrature phase of the velocity components at B-top, and the positive cospectrum values ($\langle u'v' \rangle$, shaded) indicate an offshore momentum flux. The spectrum density estimates carry 15 degrees of freedom, the effective bandwidth is 0.033 CPD, and the 95% significance level for coherence squared is shown by the horizontal arrowheads.

has been discussed in detail by BBL. The A-to-B mooring line corresponds to about the 50-km downstream coordinate distance in Figure 9*a*, indicating that the upstream meander crest was just passing over the B mooring at the time of the survey. Both of the meander crests in the February 11 view were trailing warm filaments, and the shallowness (~30 m) of their filament thermal structure is apparent on the upstream face of the view. In contrast, the cool surface water separating the filament from the main stream is indicative of isotherm uplifting that defines a cool core of water extending to greater than the 400-m depth of the AXBT survey. The positive vorticity peaks noted earlier (Figure 4) occur just after the passage of meander crests, at the times when cool cores such as those shown in Figures 7 and 9 pass over the moored array. The cyclonic circulation is consistent with that expected around a domelike structure of uplifted cool water.

The November 27 AXBT survey was completed several days after the end of the summer mooring period. However, the onshore phase (shoreward moving front) of a meander had just begun on November 25, when the instruments were retrieved. This is indicated in the 3 HRLP data (shown in referenced data reports) by increasing v and T at the B-top instrument. Two days later, at the time of the AXBT view in Figure 9*b*, the meander crest appeared to be 50–60 km downstream of the B mooring, and alternating zones of warm and cool surface waters 'behind' the meander crest, characteristic of a meander filament, are apparent near the upstream end of the view. The surface temperature contrast between the filament and the cooler water separating it from the main stream farther offshore is much smaller than it was in the winter case, because of summer warming of the coastal and shelf waters which abut the stream. The subsurface (>100 m) structure, however, was similar in both seasons. The cool core of water upstream of the meander crest is clearly evident below 100 m in the summer view.

The skewness of the meandering process, mentioned earlier, is readily apparent in the February 11 AXBT view (Figure 9*a*). It is manifested in the surface temperature, for example, by the horizontal slope of the 20°C isotherm, which is smaller downstream of the meander crest than upstream of it. The skewness is also reflected in the vertical slopes of isotherms along the downstream face of the views; namely, the isotherms move slowly downward as a crest approaches, then rapidly rise in the cool core upstream of the crest. The subsurface skewness is also clear in the late summer case (Figure 9*b*), although much of the surface temperature structure was obliterated.

5. Meander Momentum and Energy Fluxes

The u and v components of velocity at the B-top instrument were mutually coherent over the period range of 2 to 10 days in both seasons (Figure 8*c*). They were also in near quadrature over this range, with u leading v by 45°–90°, consistent with the cyclonic rotation of the velocity vector at B-top (Figure 4). The sense of the meander skewness discussed in the last section is consistent with u leading v by less than a quarter period, which implies an offshore eddy transfer of momentum. In the summer the Reynolds' stress momentum flux term $\rho\langle u'v' \rangle$ was concentrated in the 3- to 5-day period range, while in the winter it was concentrated at periods greater than about 5 days, reflecting the general seasonal differences already mentioned. The average subti-

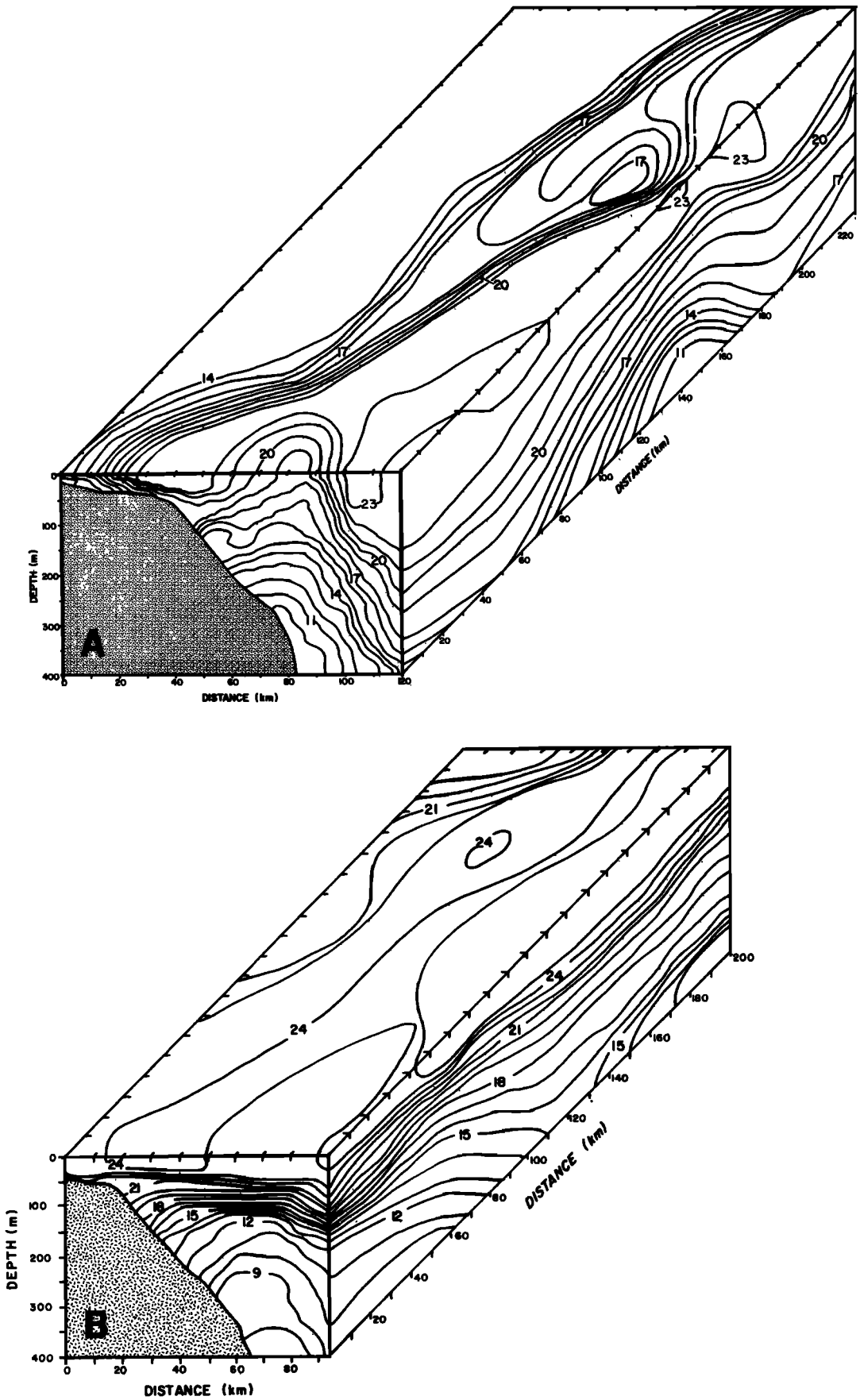

Fig. 9. Oblique views of the thermal field of the meandering Gulf Stream on (*a*) February 11, 1979, and (*b*) November 27, 1979, obtained by air-dropped expendable bathythermograph (AXBT) surveys. The February 11 case is from *Bane et al.* [1981], who give details of the survey technique and station locations. The A-to-B line in Figure 1 corresponds to the 50-km position along the downstream coordinate in this figure. The AXBT survey resolution was about 12.5 km in the offshore direction and 50 km in the downstream direction. In both views, warm filaments and cold bands are evident at the surface, adjacent to the main stream, and the uplifting of isotherms upstream of meander crests is apparent. The temperature field asymmetry in the horizontal and vertical planes is related to an offshore flux of momentum (see text).

dal value of $\langle u'v' \rangle$ determined from Figure 8 was about 100 $cm^2\ s^{-2}$ offshore in each season. This compares well with the winter estimate of (119 ± 23) $cm^2\ s^{-2}$ at B-top, calculated from the full record by direct correlation (BB81). The analogous calculation for the summer case yields (101 ± 23) $cm^2\ s^{-2}$ at B-top, insignificantly different. In both seasons, the offshore momentum flux was larger at B-top than at A-top, and the resulting divergence indicates a net retardation of the downstream current speed in the inshore edge of the mean stream, relative to offshore. Although the average value of the momentum flux was essentially the same in each season, the eddy transfer process producing the flux had shorter periods in the summer than in the winter (3 to 5 days versus >5 days, Figure 8*c*).

In the cyclonic shear zone of the mean stream, offshore momentum flux results in a transfer of kinetic energy from the fluctuations to the mean stream, via the $\rho\langle u'v' \rangle \partial\langle v \rangle / \partial x$ term in the energy equation [e.g., *Webster*, 1961*b*]. The shear of the mean stream during the Gulf Stream Meanders Experiment, calculated as $(v_{\text{B-top}} - v_{\text{A-top}})\Delta x^{-1}$, where Δx = 18 km is the mooring separation distance, was 1.05×10^{-5} s^{-1} in the winter and 1.18×10^{-5} s^{-1} in the summer. (The A-top current meter was about 150 m shallower than the B-top current meter, so the calculated mean shear is not exactly in a horizontal plane. The bottom current meter on the A mooring was not used in this calculation because of possible bottom boundary layer influences.) The corresponding energy fluxes for the full record lengths were $(125 \pm 24.3) \times 10^{-5}$ erg $cm^{-3}\ s^{-1}$ in the winter and $(120 \pm 27) \times 10^{-5}$ erg cm^{-3} s^{-1} in the summer, again insignificantly different. Taking a column-averaged mean downstream current speed of 50 cm s^{-1}, the mean kinetic energy density is 125×10^3 ergs cm^{-3}. This implies a local mean stream kinetic energy doubling time of a few weeks due to the eddy conversion process, although our data are insufficient to evaluate a cross-stream integral of the energy conversion terms. *I. H. Brooks and Niiler* [1977] found that internal readjustments within the stream resulted in no net gain of mean kinetic energy in the Florida Current. A similar calculation off North Carolina may be impossible, because of the difficulty in determining the outer 'boundary' of the stream. The surprisingly rapid local conversion of kinetic energy from the fluctuations to the mean stream in the Onslow Bay area, first noted by *Webster* [1961*b*] for the surface layer, implies an upstream or external energy source for the meanders. A more complete examination of the energetics of the stream during the winter mooring period [*Hood and Bane*, 1983] provides essentially the same conclusion.

In terms of a fluctuation stream function, ψ, the previously discussed term in the rate of energy transfer from the meanders to the mean stream can be written

$$\rho\langle u'v' \rangle \frac{\partial\langle v \rangle}{\partial x} = -\rho \left\langle \frac{\partial\psi}{\partial y} \frac{\partial\psi}{\partial x} \right\rangle \frac{\partial\langle v \rangle}{\partial x}$$

Since

$$-\frac{\partial\psi}{\partial y}\frac{\partial\psi}{\partial x} = \frac{\partial y}{\partial x}\bigg|_{\text{const } \psi} \left(\frac{\partial\psi}{\partial y}\right)^2$$

a positive average streamline slope in regions where $\partial\langle v \rangle / \partial x > 0$ indicates energy transfer from the fluctuations to the mean flow. In order for the streamline slope to be positive when averaged over a 'wave' period, the fluctuation velocity hodograph must be elliptical, with a positive major axis slope. When averaged over many wave periods, as in the winter and summer cases reported here, the positive momentum fluxes indicate that velocity fluctuations with positively skewed hodographs dominate. Two simple kinematic interpretations of the skewed, meandering, Gulf Stream front are shown in Figure 10, one for each skewness sense. The fronts are assumed to propagate toward the top of the figure ('downstream'), and the thin lines with arrowheads represent perturbation velocity streamlines. When added to a downstream current with a horizontal profile typical of the mean stream, the resulting total streamlines would show a series of cyclonic eddies along the left ('shoreward') side of each front, crudely representative of propagating Gulf Stream cool core frontal eddies. The sketches are useful because they show the consistency between the persistent offshore momentum flux noted here and the positive sense of frontal skewness (Figure 10*a*) that is most frequently observed in satellite infrared imagery [*Legeckis*, 1979] of the region off North Carolina.

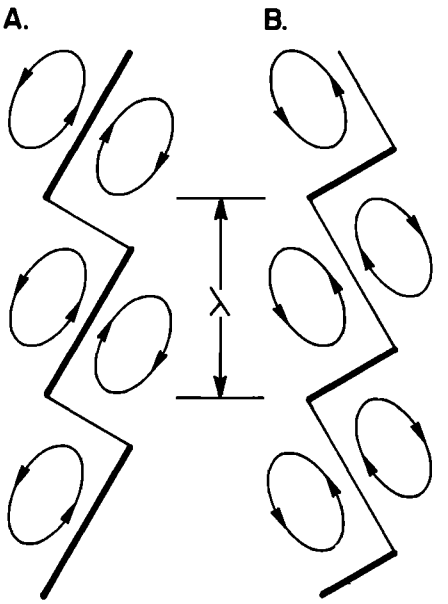

Fig. 10. Schematic perturbation streamlines showing the flow direction of two meandering fronts having the same wavelength (λ) but opposite skewness sense. The fronts propagate toward the top of the figure. (*a*) Positive skewness better conforms with the observed features of Gulf Stream meanders, in which strong surface thermal fronts (bold lines) form at an offshore location, move shoreward locally as the pattern travels downstream, and then become diffuse or reform offshore. The positive skewness of the Figure 10*a* pattern results in eddy energy transfer from the meander to the mean flow, and conversely for Figure 10*b*. A symmetric pattern would have circular streamlines and no eddy energy transfer.

6. Influence of Local Winds on Meanders

Gulf Stream fluctuations have long been associated with the winds. In his pioneering study of the Florida Current–Gulf Stream system, *Pillsbury* [1891] described the passage of an atmospheric cold front over the eastern United States, which he said caused Florida Current surface velocities that were '. . . decidedly too high.' Variable winds have been related to current fluctuations in coastal waters adjacent to Florida, Georgia, and North Carolina [*Lee and Mayer*, 1977; *Lee and Brooks*, 1979; *Janowitz and Pietrafesa*, 1980; *Hof-*

TABLE 2. First-Order Statistics for (Offshore, Longshore) Wind Stress Components From NDBO Offshore Buoy 41002 (τ_u, τ_v; dynes cm^{-2}), Wind Stress Curl ($\nabla \times \tau$; dynes cm$^{-3} \times 10^6$), and Wind Stress Divergence ($\nabla \cdot \tau$; dynes cm$^{-3} \times 10^6$)

	Minimum	Maximum	Mean	Standard Deviation
τ_u	−2.9/−2.7	3.4/3.7	0.01/−0.11	0.85/0.74
τ_v	−2.5/−3.1	4.3/3.3	0.25/0.18	0.85/0.85
$\nabla \times \tau$	−0.07/−0.05	0.07/0.07	0.02/0.03	0.04/0.04
$\nabla \cdot \tau$	−0.08/−0.07	0.06/0.05	−0.01/−0.01	0.03/0.02

Values are compared for the winter/summer mooring periods. All data were first smoothed by a 40-hour low-pass filter [from *Cohen*, 1981].

mann et al., 1981]. Direct correlations between atmospheric variables and velocity fluctuations have been found in the Florida Current [*Düing et al.*, 1977], but farther north, where the Florida continental shelf widens and the current is located farther offshore, there is a distinct drop in this correlation seaward of the 'shelf break' [*Lee and Brooks*, 1979]. This suggests that the influence of the local wind is confined to the coastal margin, where the coastal boundary can produce an effective divergence of wind-driven Ekman flux in the surface layer.

Webster [1961*a*] compared the position of the Gulf Stream front off North Carolina with the difference between the atmospheric pressure at Cape Hatteras and Charleston (Figure 1). He found a good visual correlation between the pressure difference, presumed to be proportional to the offshore geostrophic winds, and the offshore position of the front. However, he also showed that the energy the wind could be expected to contribute to the meanders was much less than the kinetic energy redistributions within the stream, and it was therefore concluded that the apparent connection between the winds and meanders might have been coincidental [*Webster*, 1961*b*].

During both field phases of the Gulf Stream Meanders Experiment, atmospheric data were collected at Cape Hatteras and at two NOAA Data Buoy Office (NDBO) offshore-moored data buoys (NDBO-2 and NDBO-4, Figure 1). These three stations were approximately located at the vertices of a right triangle, which permits finite difference computation of the wind stress curl and divergence terms in the enclosed area. The Cape Hatteras observation station is remotely located on the coastal barrier strip between Pamlico Sound and the Atlantic Ocean, which assures that all the atmospheric data were relatively free of the effects of land influences.

The raw atmospheric data consisted of hourly values of surface wind speed and direction, atmospheric pressure, and air temperature. The NDBO buoys also provided sea surface temperature. Hourly values of the wind stress vector, τ, were computed as

$$\tau = \rho_a C_D |W| (\hat{i} W_u + \hat{j} W_v)$$

where the air density at the surface was taken to be $\rho_a = 1.2 \times 10^{-3}$ g cm^{-3}, the drag coefficient $C_D = 1.5 \times 10^{-3}$, and the wind vector, **W**, has magnitude $|W|$ and components (W_u, W_v) in the ($\hat{i}$, $\hat{j}$) coordinate directions. The vector horizontal coordinate frame ($\hat{i}$, $\hat{j}$) was rotated 34° clockwise to conform with the local orientation of the 400-m isobath, such that the u component of τ and **W** is offshore and the v component of τ and **W** is in the downstream direction of the stream. In a separate calculation, the vector components of τ were computed in a nonrotated frame. The nonrotated components were used in the calculation of $\nabla \times \tau$ and $\nabla \cdot \tau$, because the meteorological stations were approximately oriented along east-west and north-south lines (Figure 1). All of the atmospheric time series were then smoothed with a 40 HRLP filter having the same response characteristic as the filter used for the moored instrument data.

The vertical component of the wind stress curl and the wind stress divergence were computed from the nonrotated wind stress vector components as follows:

$$\nabla \times \tau = \frac{\partial \tau^{(y)}}{\partial x} - \frac{\partial \tau^{(x)}}{\partial y} \doteq (\tau_2^{(y)} - \tau_4^{(y)})\Delta x^{-1} - (\tau_H^{(x)} - \tau_2^{(x)})\Delta y^{-1}$$

$$\nabla \cdot \tau = \frac{\partial \tau^{(x)}}{\partial x} + \frac{\partial \tau^{(y)}}{\partial y} \doteq (\tau_2^{(x)} - \tau_4^{(x)})\Delta x^{-1} + (\tau_H^{(y)} - \tau_2^{(y)})\Delta y^{-1}$$

In this notation, the subscripts 2, 4, H refer to atmospheric stations NDBO-2, NDBO-4, and Cape Hatteras, respectively (Figure 1); the east-west separation between NDBO-2 and NDBO-4 is Δx = 322 km, and the north-south separation between NDBO-2 and Cape Hatteras is Δy = 328 km.

First-order statistics for the low-pass-filtered wind stress and its curl and divergence are shown in Table 2, for both mooring periods. In both seasons the mean wind stress at the offshore buoy was essentially in the downstream direction. The wind stress curl and divergence fluctuated about near-zero means. The maximum wind stress of 4.3 dynes cm^{-2} (downstream) occurred in the winter, and it corresponds to a wind speed of about 20 m s^{-1} sustained for several days (i.e., over the averaging time of the low-pass filter) at the offshore NDBO buoy. The maximum values of the quantities in Table 2 are consistent with those expected for a typical extratropical cyclone northeast of Cape Hatteras [*Mooers et al.*, 1976].

Use of the unfiltered wind data would result in higher instantaneous stress estimates, but these would bias spectral transfer function calculations with the 40 HRLP currents. The work done by the wind stress on the surface currents, in a given frequency band, is equal to the dot product of the wind stress and the current speed, integrated over the duration of the stress 'event.' Exclusion of events with periods shorter than several days will bias the total work done to smaller values, but the bias is reduced by the short time scales involved. The basic 5- to 10-day synoptic scale atmospheric forcing is preserved in the 40 HRLP wind data.

The downstream (v) current and the relative vorticity fluctuations over the 200-m isobath are compared with the

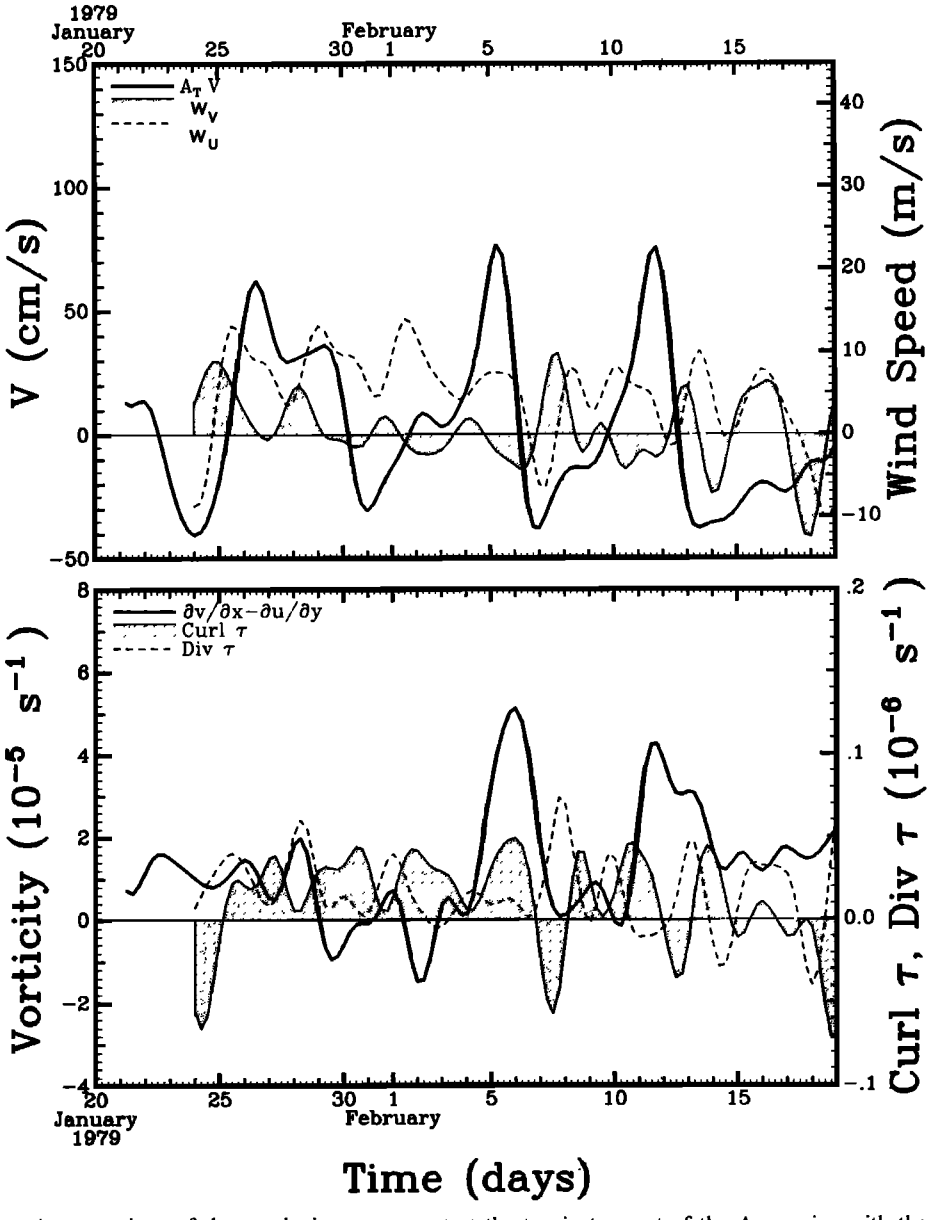

Fig. 11. A comparison of the v velocity component at the top instrument of the A mooring with the (offshore, downstream) wind component (W_u, W_v), the relative vorticity, $\zeta = \partial v/\partial x - \partial u/\partial y$, and the curl and divergence of the wind stress, τ, for the first 30 days of the winter period. All data have been 40-hour low-pass filtered.

atmospheric variables in Figure 11. The first 30 days of the 40 HRLP filtered data are shown for the winter experiment. This period was characterized by active meandering of the stream, manifested by large, weekly time scale, v component oscillations. The components of the vertical relative vorticity, $\partial v/\partial x - \partial u/\partial y$, were calculated as described in section 3. There is a similarity between the wind and the current fluctuations with time scales of 3 to 4 days. The relationship is more evident in the winter, when the clockwise-polarized downstream (W_v) and offshore (W_u) wind components are typically associated with the passage of atmospheric fronts. In the summer (not shown) the winds are more steady and generally southerly. The wind component fluctuations with 3- to 4-day periods lead the v component current fluctuations by less than 1 day in each season.

In contrast, there is little connection evident between the wind and the meander-related v component peaks which occurred on January 26 and February 5 and 11 in the winter (Figure 11), and a similar conclusion is reached for the summer case (not shown). The fluctuations associated with the meandering are distinct from the smaller-amplitude, 3- to 4-day period fluctuations.

There is also no obvious connection between the wind stress curl or divergence and the v component of the current or the relative vorticity fluctuations, in either season (Figure 11). The basis for expecting such connections is found in the vorticity and divergence equations, which show how the differential wind stresses can directly influence the ocean in the absence of coastal boundaries.

A spectral summary of the full-record relationships between wind and current fluctuations is shown for the winter case in Figures 12 and 13. The spectrum density distribution of the current fluctuations changed seasonally (Figure 8), but the coherence between the meandering currents and the wind stress was insignificant in both seasons. The spectrum density of the winter wind stress components bears little

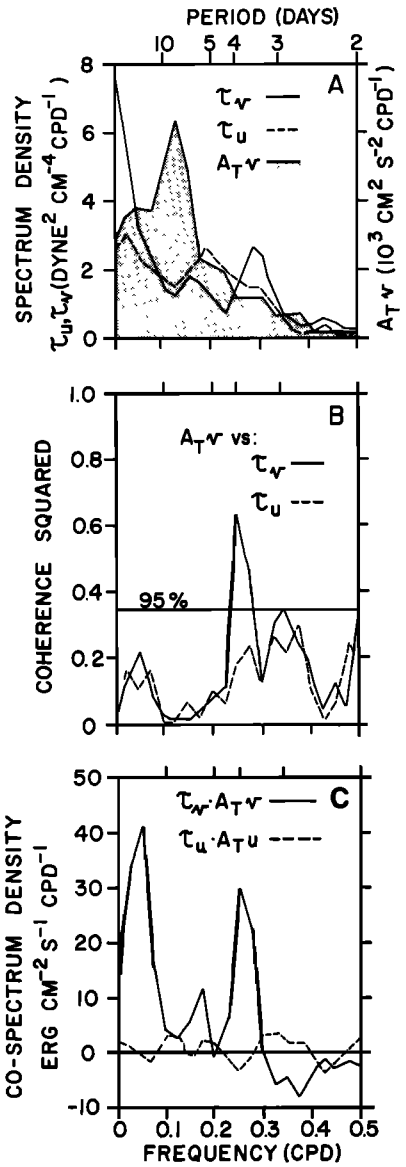

Fig. 12. (*a*) Spectrum density of wind stress components (τ_v, τ_u) at the offshore buoy NDBO-2 and the v component of the current at the A-top instrument; (*b*) coherence between the wind stress components and the A-top v component of current; (*c*) cospectrum density between the wind stress components at offshore buoy NDBO-2 and the corresponding A-top current components, with positive values indicating that the fluctuating wind is doing work on the water column. The 95% null hypothesis level is shown for coherence, and spectrum estimates carry about 15 degrees of freedom.

resemblance to the $A_T - v$ spectrum density (Figure 12*a*), and there is a pronounced coherence 'gap' between the wind stress and the current fluctuations for the 7- to 10-day period meanders (Figure 12*b*). There was, however, marginally significant coherence between the v current component and the wind stress for 3- to 4-day periods in the winter and for 2- to 3-day periods in the summer (not shown), consistent with the discussion concerning Figure 11. Examination of many other combinations of wind stress and current components from both seasons has confirmed the lack of consistent coherence for the weekly time scale meanders [*Cohen*, 1981].

The wind stress curl and divergence were marginally coherent with the current fluctuations only in the 3- to 4-day period band (Figure 13). In contrast with the wind stress, the spectrum of the wind stress curl has a peak that corresponds with the $A_T - v$ peak at a period of ~9 days, but there is only a suggestion of enhanced coherence between the fluctuating currents and the wind stress curl in the 7- to 10-day period band. Overall, the differential wind stress forcing mechanism was found to be somewhat more effective than the direct action of the wind stress, but a consistent and convincing relationship was not found [*Cohen*, 1981].

The essential independence of the wind and current fluctuations off North Carolina can be demonstrated from the rate of working of the wind stress on the currents. Ideally, an estimate of this quantity would require the measurement of surface currents, which are not available in the present case. However, the high vertical coherence and in-phase nature of the fluctuations can be exploited, allowing the rate of working to be calculated using a middepth current record. The result, which can be interpreted as a column-averaged estimate of the downstream rate of working in each frequency band, is the cospectrum between the v component of the wind stress and the v component of the current fluctuations. A winter example is shown in Figure 12*c* for the A mooring. Positive values in period bands of significant coherence indicate work being done on the current by the wind. This occurred only in the downstream direction, and only for the 3- to 4-day period band in the winter. The cross-stream rate of working was insignificant.

The peak value of the coherent downstream cospectrum occurs at a period of 4 days in Figure 12*c*. Multiplying the peak value by the peak bandwidth (~0.05 CPD) yields ~1.5 ergs cm^{-2} s^{-1} as the average rate of working on the column by the wind, per unit surface area, or 4.5×10^6 ergs cm^{-1} s^{-1} as the average rate in a 30-km-wide cross-shelf scale width.

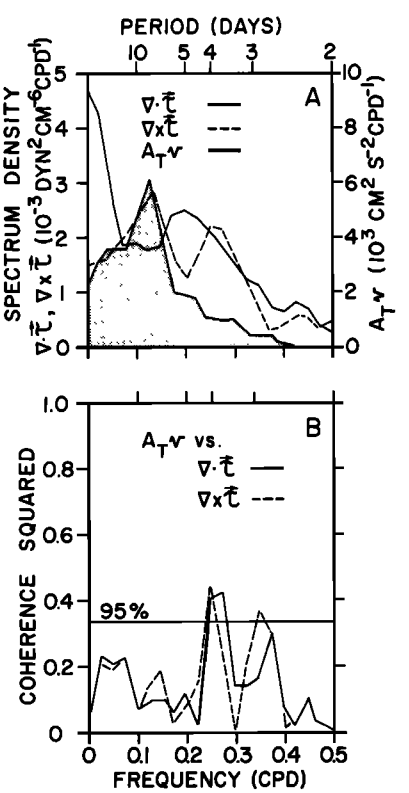

Fig. 13. As in Figures 12*a* and 12*b*, except comparing wind stress divergence and curl with the A-top v current component.

For a mean stream velocity of 0.5 m s^{-1} in the top 100 m of the 30-km-wide strip, the mean kinetic energy density is 7.5 $\times 10^{13}$ ergs cm^{-1}, which implies a wind-driven mean kinetic energy doubling time of ~0.5 yr. This can be compared to the doubling time of a few weeks indicated in the preceding section by the rate of kinetic energy eddy transfer from the fluctuating currents to the mean stream. The marginal coherence between the wind and the 3- to 4-day period current fluctuations (Figure 12*b*) is therefore probably not a result of wind forcing at the moored array site; rather, it may be a vestigial indication that the wind forcing was effective at 3- to 4-day periods in the near-shore zone, shoreward of the moorings. The cross-shelf scale within which the coastal wind forcing mechanism is expected to be effective off North Carolina is ~30 km [*Chao and Pietrafesa,* 1980]. The A mooring was several times this distance from the coast.

7. Summary Discussion

Gulf Stream meanders were prominent during most of the 4-month winter and summer mooring periods of the Gulf Stream Meanders Experiment. In both seasons, the mid-depth current speeds over the 400-m isobath typically fluctuated between −50 cm s^{-1} and +100 cm s^{-1} relative to a mean value of 30 cm s^{-1} in the downstream direction. In the winter (January to May) the velocity, temperature, and salinity fluctuations had a prominent period of 7 to 10 days and a less prominent period of 3 to 4 days. In the summer (July to November) the fluctuations had less well-defined time scales within a generally energetic 3- to 10-day period band. The subtidal velocity fluctuations were highly coherent and nearly in phase vertically throughout the lower half of the water column. They were also coherent over the downstream scale of the array (64 km), with an indicated downstream propagation speed of ~40 km d^{-1} in both seasons.

The fluctuations of the stream known as meanders extended to near bottom in both seasons. Based on temperature measurements, *Webster* [1961*a*] described meanders in the upper 200 m as lateral, wavelike, downstream propagating excursions of the Gulf Stream front having a prominent weekly time scale. Our more extensive surveys of the current, temperature, and salinity signatures of meanders support Webster's description, although the structure is more complicated along the shoreward edge of the stream, where shallow surface filaments of warm water often trail southwestward from meander crests. Strong cyclonic rotation of the velocity vectors at individual instruments is characteristically observed just after the passage of a meander crest. The cyclonic rotation, which is also clearly a bulk property of the water motions, is associated with deep uplifting or upwelling of cool water from within the stream upstream of meander crests. The intensity of the meander process is often sufficient to bring cool water to the surface, producing longshore bands or streaks of cool water separating the warm filaments from the stream farther offshore. The cyclonic circulation around the resulting dome of cool water is often strong enough to produce countercurrents (i.e., upstream or southwestward flow) of 50 cm s^{-1} under the warm filaments. It seems likely that similar countercurrents prompted White's cautionary remark in 1590 about Gulf Stream eddies off the Carolinas.

The fundamental energy source of the meanders is still unclear. Meanders were common in both seasons, but their attendant weekly time scale, sharply defined in the winter, was blurred into a broader band of energetic fluctuations in the summer. The leading term in the energy equation, evaluated for each season, indicated a conversion of fluctuation kinetic energy to mean stream kinetic energy. The conversion process is associated with the lateral asymmetry or skewness of the meanders, commonly observed in the surface and subsurface thermal structure of the stream. The sense of the skewness, indicated by a relatively gentle shoreward approach of the Gulf Stream front followed by a more abrupt offshore displacement, is consistent with decreasing meander kinetic energy. The Reynolds' stress term responsible for the energy conversion, $\rho\langle u'v'\rangle$, had about the same subtidal average value in each season, but the associated eddy process had significantly shorter periods in the summer than in the winter.

The local wind stress and its curl and divergence were essentially unrelated to the weekly time scale meanders, in either season. There was marginal correlation between the winds and currents for 3- to 4-day periods in the winter only, but the rate of working on the currents by the wind stress was insignificant in both seasons, compared with the indicated energy exchanges within the stream.

Our observations were limited to the lower half of the water column, in the inshore flank of the stream. Consequently, it is premature to draw firm conclusions about the source and fate of meanders off North Carolina. Nevertheless, the results presented here complement and extend earlier ideas, which, viewed collectively, point to a seasonally independent meander energy source upstream of the Onslow Bay area. As noted by many others, it seems likely that the meanders evolve from an instability of the stream, but the details of where and how this happens are still developing. The frontal disturbances which eventually grow into meanders are evident in the Florida Current, but their roots may be traceable back even to the Loop Current in the Gulf of Mexico. The rapid meander amplification associated with the stream deflection off Charleston seems to mark the end of their growth phase, perhaps because the joint configuration of the stream and the bottom topography downstream of the deflection region is no longer unstable to perturbations having the space and time scales of meanders.

A clearer understanding of the difficult but fascinating energy history of meanders will evolve as more sophisticated observation techniques become available. The prospect of large-scale, satellite altimetric measurements of surface currents seems especially promising for future studies of Gulf Stream meanders.

Acknowledgments. We are pleased to acknowledge the joint project support of the National Science Foundation, grants OCE 77-25682 and OCE 79-06710, and the Office of Naval Research, contract N 00014-77-C-0354. Since the inception of the Gulf Stream Meanders Experiment in 1976, many individuals, too numerous to mention here but acknowledged in previous papers, have made valuable contributions of time, labor, and thought. We are especially indebted to Paul Blankinship, of North Carolina State University, for his meticulous preparation of instruments. The high percentage of data returned without the loss of a single instrument attests to his carefulness. We also thank Captain Herb Bennett and the crew of R/V *Endeavor* for contributing to four successful and enjoyable cruises in the Gulf Stream in 1979. Aircraft time for the AXBT flights was provided by the U.S. Naval Oceanographic Office. The atmospheric data sets were organized by R. Cohen, and the statistics in Table 2 were condensed from his master's thesis, which was supported by National Science Foundation grant OCE 79-06710. In

retrospect, it appears that more questions about meanders have been raised than answered. We hope that these questions will provide a provocative incentive for continuing study of the Gulf Stream.

REFERENCES

Bane, J. M., Jr., and D. A. Brooks, Gulf Stream meanders along the continental margin from the Florida Straits to Cape Hatteras, *Geophys. Res. Lett.*, *6*(4), 280–282, 1979.

Bane, J. M., Jr., D. A. Brooks, and K. R. Lorenson, Synoptic observations of the three-dimensional structure and propagation of Gulf Stream meanders along the Carolina continental margin, *J. Geophys. Res.*, *86*(C7), 6411–6425, 1981.

Brooks, D. A., and J. M. Bane, Jr., Gulf Stream fluctuations and meanders over the Onslow Bay upper continental slope, *J. Phys. Oceanogr.*, *11*, 247–256, 1981.

Brooks, D. A., J. M. Bane, Jr., R. L. Cohen, and P. Blankinship, The Gulf Stream Meanders Experiment: Current meter and atmospheric data report for the August to November 1979 mooring period, *Rep. 81-3-T*, Tex. A&M Univ., College Station, 1981.

Brooks, I. H., and P. P. Niiler, Energetics of the Florida Current, *J. Mar. Res.*, *35*, 163–191, 1977.

Chao, S.-Y., and L. J. Pietrafesa, the subtidal response of sea level to atmospheric forcing in the Carolina Capes, *J. Phys. Oceanogr.*, *10*, 1246–1255, 1980.

Cohen, R. L., Atmospheric influences on Gulf Stream fluctuations off Onslow Bay, North Carolina, M.S. thesis, 41 pp., Tex. A&M Univ., College Station, 1981.

DeVorsey, L., Pioneer charting of the Gulf Stream: The contributions of Benjamin Franklin and William Gerard de Brahm, *Imago Mundi*, *28*(2), 105–120, 1976.

Düing, W. O., C. N. K. Mooers, and T. N. Lee, Low-frequency variability in the Florida Current and relations to atmospheric forcing from 1972 to 1974, *J. Mar. Res.*, *35*, 129–161, 1977.

Herrera y Tordesillas, Antonio de, Historia general de los hechos de los Castellanos en las islas i tierra firme del Mar Oceano, 5 vols., Emprenta real, por Iuan Flamenco, Madrid, 1601.

Hofmann, E. E., L. J. Pietrafesa, and L. P. Atkinson, A bottom water intrusion in Onslow Bay, North Carolina, *Deep Sea Res.*, *28A*, 329–345, 1981.

Hood, C. A., and J. M. Bane, Jr., Subsurface energetics of the Gulf Stream cyclonic frontal zone off Onslow Bay, North Carolina, submitted to *J. Geophys. Res.*, 1983.

Ignaszewski, M., The vorticity balance of Gulf Stream meanders off North Carolina, M.S. thesis, Tex. A&M Univ., College Station, 1982.

Janowitz, G. S., and L. J. Pietrafesa, A model and observations of time dependent upwelling over the mid-shelf and slope, *J. Phys. Oceanogr.*, *10*, 1574–1583, 1980.

Lee, T. N., and D. A. Brooks, Initial observations of current, temperature and coastal sea level response to atmospheric and Gulf Stream forcing on the Georgia shelf, *Geophys. Res. Lett.*, *6*, 321–324, 1979.

Lee, T. N., and D. A. Mayer, Low-frequency current variability and spin-off eddies along the shelf off southeast Florida, *J. Mar. Res.*, *35*, 193–220, 1977.

Lee, T. N., L. P. Atkinson, and R. Legeckis, Detailed observations of a Gulf Stream frontal eddy on the Georgia continental shelf, April 1977, *Deep Sea Res.*, *28A*(4), 347–375, 1981.

Legeckis, R. V., Satellite observations of the influence of bottom topography on the seaward deflection of the Gulf Stream off Charleston, South Carolina, *J. Phys. Oceanogr.*, *9*, 483–497, 1979.

Mooers, C. N. K., J. Fernandez-Partagas, and J. F. Price, Meteorological forcing fields of the New York Bight (first year), *Tech. Rep. TR76-8*, Mar. Stud. Center, Univ. of Del., Dover, 1976.

Pillsbury, J. E., The Gulf Stream, for year ending June 1890, rep. supp., append. 10, U.S. Coastal and Geod. Surv., Washington, D.C., 1891.

Quinn, D. (Ed.,), *The Roanoke Voyages*, vol. 2, p. 608, The Hakluyt Society, London, 1952.

Richardson, P. L., Benjamin Franklin and Timothy Folger's first printed chart of the Gulf Stream, *Science*, *207*, 643–645, 1980.

Richardson, W. S., W. J. Schmitz, and P. P. Niiler, The velocity structure of the Florida Current from the Straits of Florida to Cape Fear, *Deep Sea Res.*, *16*, 225–231, 1969.

Scisco, L. D., The track of Ponce de Leon in 1513, *Bull. Am. Geogr. Soc.*, *XLV*(10), 721–735, 1913.

Stommel, H., *The Gulf Stream*, 248 pp., University of California Press, Berkeley, 1966.

von Arx, W. S., D. F. Bumpus, and W. S. Richardson, On the fine-structure of the Gulf Stream front, *Deep Sea Res.*, *3*, 46–55, 1955.

Webster, F., A description of Gulf Stream meanders off Onslow Bay, *Deep Sea Res.*, *9*, 130–143, 1961*a*.

Webster, F., The effect of meanders on the kinetic energy balance of the Gulf Stream, *Tellus*, *13*, 392–401, 1961*b*.

(Received March 25, 1982;
revised September 3, 1982;
accepted September 3, 1982.)